This article has been accepted for publication in a future issue of this journal, but has not been fully edited. Content may change prior to final publication. Citation information: DOI 10.1109/TVT.2014.2298232, IEEE Transactions on Vehicular Technology

Simplified Parallel Interference Cancelation for Under-Determined MIMO Systems

Chen Qian, Jingxian Wu, *Member, IEEE*, Yahong Rosa Zheng, *Senior Member, IEEE*, and Zhaocheng Wang, *Senior Member, IEEE*

***Abstract*—A low complexity detection scheme is proposed in this paper for under-determined multiple-input multiple-output (UD-MIMO) wireless communication system that employs N transmit antennas and $M < N$ receive antennas. The proposed scheme combines a simplified parallel interference cancelation (S-PIC) with the block decision feedback equalization (BDFE) algorithm. To account for the extra $(N - M)$-dimension in the transmitted signal, the UD-MIMO system is partitioned into two subsystems, one with $(N - M)$ transmit antennas and the other one with M transmit antennas. The interference from the first subsystem to the second one is canceled in parallel and BDFE is performed over the second subsystem. Unlike conventional PIC methods that exhaustively search all the $Q^{(N-M)}$ sequences in the first subsystem, with Q being the constellation size, the proposed scheme explores only a small number of candidate sequences in the first subsystem, thus achieves significant complexity reduction. Two new candidate sequence selection methods are proposed. In the first iteration, the candidate sequences used for PIC are selected by exploring the statistical properties of the received signals. In the second iteration and beyond, the set containing the candidate sequences is constructed by utilizing the soft information generated from the previous iteration. The proposed scheme provides a balanced tradeoff between computational complexity and bit error rate (BER) performance.**

***Index Terms*—Under-determined multiple-input multiple-output (UD-MIMO), turbo detection, parallel interference cancelation (PIC), block decision feedback equalization (BDFE), wireless communication.**

I. Introduction

Consider a multiple-input multiple-output (MIMO) communication system that employs N transmit antennas and M receive antennas. A MIMO system is symmetric if $N = M$ or over-determined if $N < M$, and they are referred to as conventional MIMO systems in this paper. In many practical applications, there are more transmit antennas available than receive antennas, and such systems with spatial multiplexing are referred to as under-determined (UD) MIMO or overloaded MIMO systems. For example, in the downlink of cellular systems, the base station often has a large number of transmit antennas while the mobile station is usually equipped with a small number of receive antennas. In the uplink multi-user transmission, when the number of users exceeds the number of receive antenna at the base station, the system can also be treated as UD-MIMO. In vehicular infotainment systems [1], more antennas can be installed in the roadside infrastructure than those on the vehicles, forming a UD-MIMO system that can achieve a higher data rate than conventional MIMO systems. The constantly increasing demand for high data rate communications over scarce spectrum resources motivates the development of communication systems that can effectively exploit the multiplexing gains of UD-MIMO systems.

Similar to a conventional MIMO system, the optimal detection in a UD-MIMO system uses the maximum likelihood (ML) or maximum *a posteriori* probability (MAP) detection that performs an exhaustive search over all the possible Q^N transmitted vectors, where Q is the modulation constellation size. However, the computational complexity of the ML and MAP detectors grows exponentially with Q and N, making them prohibitive for practical implementations when Q or N is large. Therefore, the optimal detectors are only used for small UD-MIMO systems [2], [3]. Many sub-optimal solutions originally developed for conventional MIMO systems are recently extended to UD-MIMO systems. For example, the recursive Tabu search (RTS) algorithm [4], [5] has been applied to large UD-MIMO systems in [6], where a random initial vector is used as a starting point to perform heuristic local search of a tree structure. Alternatively, the sphere decoding (SD)-based algorithms [7], [8] have been applied to UD-MIMO by different approaches, such as the slab SD [9], [10], the generalized SD (GSD) [11]–[15], the center-shifting K-best algorithm [16], the λ-GSD [17], and the two-stage LSD [18]. Most SD-based algorithms have to combat the problem that the channel Gram matrix is rank-deficient and the initial estimate cannot be obtained directly. Other low-complexity MIMO detectors, such as the ordered successive interference cancelation (OSIC) or the vertical Bell laboratories layered space-time (V-BLAST) [19], also suffer from the rank-deficiency problem when applied to UD-MIMO systems [20], [21].

Three remedies are found in the literature to overcome the rank-deficiency problem in UD-MIMO detections. One is to partition the UD-MIMO system into Q^D parallel symmetric subsystems [11], where $D = N - M$ is the difference in

Copyright © 2013 IEEE. Personal use of this material is permitted. However, permission to use this material for any other purposes must be obtained from the IEEE by sending a request to pubs-permissions@ieee.org.

The work of Chen Qian and Zhaocheng Wang was supported by National 973 Program of China (Grant No. 2013CB329203), National Nature Science Foundation of China (Grant No. 61271266), National High Technology Research and Development Program of China (Grant No. 2012AA011704) and the ZTE fund project CON1307250001. The work of Yahong Rosa Zheng was supported in part by National Science Foundation of the USA under Grant ECCS-0846486. The work of Jingxian Wu was supported in part by the National Science Foundation of the USA under Grant ECCS-1202075.

Chen Qian and Zhaocheng Wang are with Tsinghua National Laboratory for Information Science and Technology (TNList), Department of Electronic Engineering, Tsinghua University, Beijing 100084, China (e-mail: qc8802@gmail.com; zcwang@mail.tsinghua.edu.cn).

Jingxian Wu is with Department of Electrical Engineering, University of Arkansas, Fayetteville, AR 72701, USA (e-mail: wuj@uark.edu).

Yahong Rosa Zheng is with Department of Electrical and Computer Engineering, Missouri University of Science and Technology, Rolla, MO 65409, USA (e-mail: zhengyr@mst.edu).

0018-9545 (c) 2013 IEEE. Personal use is permitted, but republication/redistribution requires IEEE permission. See http://www.ieee.org/publications_standards/publications/rights/index.html for more information.

This article has been accepted for publication in a future issue of this journal, but has not been fully edited. Content may change prior to final publication. Citation information: DOI 10.1109/TVT.2014.2298232, IEEE Transactions on Vehicular Technology

transmit-receive antenna numbers. This partitioning usually requires exhaustive search over the Q^D dimensions [11], and it suffers from high complexity when D is large. Alternatively, a 2-layered or multi-layered partitioning is applied to the QR-decomposed channel matrix in [12] or [13], which leads to a 2-stage or multi-depth SD. The second remedy is to modify the Gram matrix with diagonal loading [14], [16], [18] such that the matrix can be inverted to yield the initial estimates. The diagonal loading used in [14], [16] results in a biased estimation and requires center shifting [16] if the K-best algorithm is used; while our recent work [18] modifies the loading and the conventional list sphere decoding (LSD) to achieve good performance and low complexity simultaneously. The third remedy to the rank-deficiency problem is to transform the channel matrix directly into full rank by either adding a λ loading [17] or by oversampling the receiver with offset transmission to create additional "virtual" receiver elements that resemble the conventional MIMO channel matrix [20].

This paper proposes a low-complexity iterative algorithm for UD-MIMO detection, which combines a simplified parallel interference cancelation (S-PIC) with soft block decision feedback equalization (BDFE) [22]. The proposed S-PIC-BDFE scheme is based on the generalized parallel interference cancelation (GPIC) scheme proposed in [23] and partitions the UD-MIMO system into two subsystems $\mathbf{H}_1$ and $\mathbf{H}_2$ of sizes $D \times M$ and $M \times M$, respectively, which is the same as in [11]. However, unlike [11] and [23] that perform exhaustive search over all the Q^D possible sequences corresponding to $\mathbf{H}_1$, the proposed scheme only selects a small number of the most probable candidate sequences from subsystem $\mathbf{H}_1$, and they are treated as interference to the symmetrical subsystem $\mathbf{H}_2$. After parallel cancelation of all the interferences, multiple subsystems with channel matrix $\mathbf{H}_2$ are created and are detected in parallel by the BDFE algorithm [22]. The performance of the UD-MIMO system improves as soft information is exchanged between the UD-MIMO detector and channel decoder through iterations.

One of the main contributions of the proposed scheme is the S-PIC, which achieves significant complexity reduction by selecting a small number of candidate sequences from subsystem $\mathbf{H}_1$. We propose two different candidate selection methods, one for the first iteration without *a priori* information, another for the second and later iterations when log-likelihood ratios (LLRs) from the previous iteration are available. Both selection methods ensure that the truly transmitted sequence is included in the candidate sequence set with a very high probability. As a result, the performance of the S-PIC is almost identical to PIC with exhaustive search, but with a much lower complexity. Our PIC approach differs from [23], [24] in that a reduced set of candidates are considered for interference cancelation rather than the whole set of candidates; our PIC approach also differs from [25] in that complete cancelation of interference is used for all iterations rather than the partial cancelation in [25]. We demonstrate that the PIC approach exhibits better BER performance than OSIC for UD-MIMO. The utilization of BDFE instead of the zero-forcing or minimum mean square error (MMSE) detector for subsystem $\mathbf{H}_2$ also improves the performance considerably. A brief analysis on computational complexity is also provided.

Common notations used in this paper are listed here. $\mathcal{CN}(\mu, \sigma^2)$ denotes the complex Gaussian distribution with mean μ and variance σ^2; $F_X(x)$ denotes the cumulative distribution function (CDF) of the random variable X; $P(x)$ denotes the probability of event x; $\mathcal{C}^{M\times N}$ and $\mathcal{R}^{M\times N}$ denote the $M \times N$ dimensional complex- and real-number space, respectively; $E[\cdot]$ is the expectation operator; $\mathbf{I}_M$ denotes the identity matrix of size M; $\det(\cdot)$ is the matrix determinant operator; and $\text{Diag}(a_1, \cdots, a_m, \cdots, a_M)$ denotes a diagonal matrix with the m-th diagonal element being a_m. The superscripts $()^T$ and $()^H$ denote the matrix transpose and the matrix Hermitian, respectively.

II. System Model and Turbo Detection

A UD-MIMO system with N transmit antennas and M receive antennas is depicted in Fig. 1, where $N > M$ and $h_{mn} \sim \mathcal{CN}(0, 1)$ is the baseband equivalent channel coefficient between the n-th transmit antenna and the m-th receive antenna. The N independent bit streams $\{\mathbf{a}_n\}_{n=1}^N$ are encoded by channel encoders to generate the coded bit streams $\{\mathbf{b}_n\}_{n=1}^N$. The coded bit streams are interleaved by pseudo-random interleavers to obtain the interleaved bit streams $\mathbf{c}_n = \Pi(\mathbf{b}_n)$, for $n = 1 \cdots N$, where $\Pi(\cdot)$ is the interleaving operator. Then every P bits are mapped to a symbol in the modulation constellation set $\mathcal{S}$ that has a cardinality $Q = 2^P$. The modulated symbol vectors, $\mathbf{s} = [s_1, \cdots, s_N]^T \in \mathcal{S}^{N\times 1}$, are transmitted by N antennas through a channel with flat fading and additive white Gaussian noise (AWGN). The total energy of all the N transmitted symbols is $E_s = E[\mathbf{s}^H\mathbf{s}]$.

Denote the $M \times N$ channel matrix as $\mathbf{H}$ with h_{mn} on the m-th row and the n-th column of $\mathbf{H}$, and the complex AWGN vector as $\mathbf{v} = [v_1, \cdots, v_M]^T \in \mathcal{C}^{M\times 1}$ with $v_m \sim \mathcal{CN}(0, \sigma_0^2)$. Denote the received baseband-equivalent signal as $\mathbf{y} = [y_1, \cdots, y_M]^T \in \mathcal{C}^{M\times 1}$, then we have the UD-MIMO system model

$$\mathbf{y} = \mathbf{H}\mathbf{s} + \mathbf{v}. \tag{1}$$

It is assumed that the channel matrix $\mathbf{H}$ is known at the receiver.

For the receiver, the optimum UD-MIMO detector may employ the turbo detection similar to that in conventional MIMO receivers, also shown in Fig. 1, where a MIMO soft-symbol detector and N soft channel decoders are connected by de-interleavers and interleavers. Soft information is iteratively exchanged between the soft-symbol detector and the soft channel decoders. The MIMO symbol detector generates the soft *a posteriori* LLRs $L_{D1}^{n,p}$ for the coded bit $c_{n,p}$, where the superscripts p and n denote the p-th bit from the n-th transmit antenna. The extrinsic LLRs are calculated as $L_{E1}^{n,p} = L_{D1}^{n,p} - L_{A1}^{n,p}$, where $L_{A1}^{n,p}$ is the soft *a priori* LLR for the bit $c_{n,p}$. The extrinsic LLR $L_{E1}^{n,p}$ is deinterleaved to yield the soft *a priori* LLR $L_{A2}^{n,p}$ for the channel decoder, that is, $L_{A2}^{n,p} = \Pi^{-1}(L_{E1}^{n,p})$, where $\Pi^{-1}(\cdot)$ is the deinterleaving operator. Using $L_{A2}^{n,p}$ as the input, the channel decoder generates the soft *a posteriori* LLR $L_{D2}^{n,p}$ and the extrinsic LLR $L_{E2}^{n,p}$. Then $L_{E2}^{n,p}$ is interleaved to generate the soft *a priori* LLR $L_{A1}^{n,p} = \Pi(L_{E2}^{n,p})$, which is used as the input to the soft symbol

0018-9545 (c) 2013 IEEE. Personal use is permitted, but republication/redistribution requires IEEE permission. See http://www.ieee.org/publications_standards/publications/rights/index.html for more information.

This article has been accepted for publication in a future issue of this journal, but has not been fully edited. Content may change prior to final publication. Citation information: DOI 10.1109/TVT.2014.2298232, IEEE Transactions on Vehicular Technology

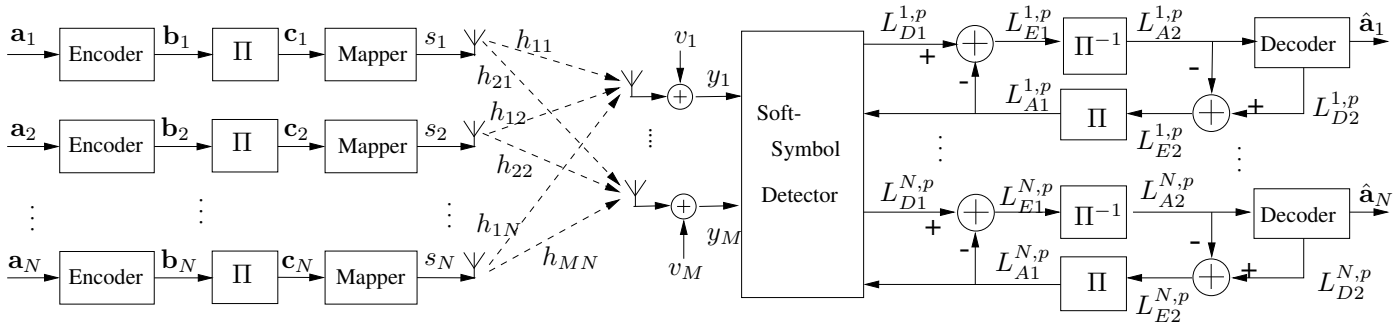

Fig. 1. UD-MIMO transceiver with turbo iterative detection, where Π and Π^{-1} denote the interleaver and the deinterleaver, respectively.

detector for the next iteration. For the first iteration, $L_{A1}^{n,p}=0$ since there is no *a priori* information.

In the soft MIMO symbol detector, the soft *a posteriori* LLR $L_{D1}^{n,p}$ for bit $c_{n,p}$ is calculated as

$$L_{D1}^{n,p}=\ln\frac{\sum_{\mathbf{s}\in\mathcal{S}_{n,p,0}}\exp\left(-\frac{1}{\sigma_0^2}\|\mathbf{y}-\mathbf{H}\mathbf{s}\|^2\right)P(\mathbf{s})}{\sum_{\mathbf{s}\in\mathcal{S}_{n,p,1}}\exp\left(-\frac{1}{\sigma_0^2}\|\mathbf{y}-\mathbf{H}\mathbf{s}\|^2\right)P(\mathbf{s})}, \tag{2}$$

where $\mathcal{S}_{n,p,b}$ contains all the possible transmitted vectors in the set $\mathcal{S}^{N\times 1}$ with $c_{n,p}=b$ for $b=0,1$ and $P(\mathbf{s})$ denotes the *a priori* probability for the vector $\mathbf{s}$. The optimal solution to (2) requires an exhaustive search over the whole set $\mathcal{S}^{N\times 1}$, resulting in a complexity on the order of $\mathcal{O}(Q^N)$. The exponentially grown complexity of the optimal detector makes it difficult to implement in practical systems, even for moderate Q and N. Although many sub-optimal solutions based on sphere decoding are developed for UD-MIMO systems, the computational complexity of those algorithms is still pretty high, especially when $N-M$ is large.

III. Simplified Parallel Interference Cancelation with BDFE

A S-PIC scheme is proposed for iterative UD-MIMO detection, which combines a low-complexity PIC with BDFE, as shown in Fig. 2.

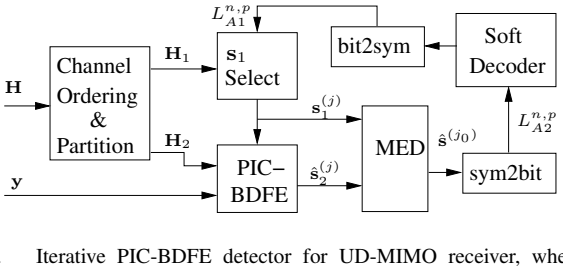

Fig. 2. Iterative PIC-BDFE detector for UD-MIMO receiver, where the sym2bit block contains soft symbol to bit LLR calculation and de-interleaver, and the bit2sym block contains interleaver and bit LLR to soft symbol mapping.

In the first iteration, the columns of the channel matrix are sorted in an ascending order based on the Frobenius norms of the rows of the pseudo-inverse of $\mathbf{H}$ [23], as $\|\left(\mathbf{H}^{\dagger}\right)_k\|$, where the superscript $()^{\dagger}$ denotes matrix pseudo-inverse, the subscript $(\mathbf{H})_k$ represents the k-th row of the matrix $\mathbf{H}$, and $\|\cdot\|$ is the Frobenius norm of a vector. The channel matrix with the ordered columns is then partitioned into two matrices as $\mathbf{H}_1=[\mathbf{h}_{i_1},\cdots,\mathbf{h}_{i_D}]\in\mathcal{C}^{M\times D}$ and $\mathbf{H}_2=[\mathbf{h}_{i_{D+1}},\cdots,\mathbf{h}_{i_N}]\in\mathcal{C}^{M\times M}$, where $D=N-M$, the ordered index set $\{i_1,\cdots,i_N\}$ are a permutation of $\{1,\cdots,N\}$ and $\mathbf{h}_{i_n}$ is the i_n-th column of $\mathbf{H}$.

After the partition, the UD-MIMO system in (1) is equivalently represented as the superposition of a $D\times M$ system and an $M\times M$ system as

$$\mathbf{y}=\mathbf{H}_1\mathbf{s}_1+\mathbf{H}_2\mathbf{s}_2+\mathbf{v}, \tag{3}$$

where $\mathbf{s}_1=[s_{i_1},\cdots,s_{i_D}]^T\in\mathcal{S}^{D\times 1}$ and $\mathbf{s}_2=[s_{i_{D+1}},\cdots,s_{i_N}]^T\in\mathcal{S}^{M\times 1}$. Note that even though $\mathbf{H}_2$ is a equivalent channel matrix of a symmetric MIMO, $\mathbf{H}_1$ may still be under-determined depending on D and M. The partitioning is the same as that in [11], [21].

The number of possible $\mathbf{s}_1$ vectors is Q^D. Denote the Q^D possible values of $\mathbf{s}_1$ as $\{\mathbf{s}_1^{(j)}\}_{j=1}^{Q^D}$. In the proposed method, only a small number of the most probable candidates of $\mathbf{s}_1$ are selected to form a candidate set, denoted as $\left\{\mathbf{s}_1^{(j)}|j\in\mathcal{J}\right\}$, where the set $\mathcal{J}$ with cardinality J is the candidate index set. Each particular sequence $\mathbf{s}_1^{(j)}$ is treated as an interference to the symmetrical subsystem $\mathbf{H}_2\mathbf{s}_2^{(j)}$ and can be canceled to yield an equivalent system

$$\mathbf{y}_j=\mathbf{y}-\mathbf{H}_1\mathbf{s}_1^{(j)}=\mathbf{H}_2\mathbf{s}_2^{(j)}+\mathbf{v},\quad j\in\mathcal{J}. \tag{4}$$

The parallel cancelation of all the interferences results in multiple subsystems in the form of (4). These symmetric subsystems are detected in parallel by the BDFE algorithm [22] to yield the corresponding $\hat{\mathbf{s}}_2^{(j)}$. Since no *a priori* information is available at the first iteration, the $\mathbf{s}_1^{(j)}$ selection and the BDFE detection for the first iteration are different from those for the second iteration and beyond. The following subsections will present the details of the BDFE detection and candidate set selection for the various iterations.

A. The First Iteration

The BDFE performs a sequence-based detection for the symmetrical subsystem (4) through two block filters [22]: a feedforward filter, $\mathbf{W}\in\mathcal{C}^{M\times M}$, and a strict upper triangular feedback filter with zero diagonal elements, $\mathbf{B}\in\mathcal{C}^{M\times M}$. In the first iteration, no *a priori* information is available for either $\mathbf{s}_1$ or $\mathbf{s}_2$. Therefore, the BDFE filters derived by following the

0018-9545 (c) 2013 IEEE. Personal use is permitted, but republication/redistribution requires IEEE permission. See http://www.ieee.org/publications_standards/publications/rights/index.html for more information.

This article has been accepted for publication in a future issue of this journal, but has not been fully edited. Content may change prior to final publication. Citation information: DOI 10.1109/TVT.2014.2298232, IEEE Transactions on Vehicular Technology

MMSE criterion are the same for all the J parallel subsystems. That is

$$\begin{aligned}\mathbf{B} &= \mathbf{U}-\mathbf{I}_M,\\ \mathbf{W} &= \mathbf{U}\mathbf{H}_2^H\left(\mathbf{H}_2\mathbf{H}_2^H+\sigma_0^2\mathbf{I}_M\right)^{-1}\end{aligned} \tag{5}$$

where $\mathbf{U}\in\mathcal{C}^{M\times M}$ is an upper triangular matrix with unit diagonal elements. The matrix $\mathbf{U}$ is obtained from the Cholesky decomposition as

$$\frac{1}{E_s}\mathbf{I}_M+\frac{1}{\sigma_0^2}\mathbf{H}_2^H\mathbf{H}_2=\mathbf{U}^H\mathbf{\Delta}\mathbf{U},$$

where σ_0^2 is the noise variance and $\mathbf{\Delta}\in\mathcal{R}^{M\times M}$ is a diagonal matrix. It is clear that the two filters defined in (5) depend only on the channel matrix $\mathbf{H}_2$.

The j-th BDFE detector outputs the soft symbol sequence $\hat{\mathbf{s}}_2^{(j)}$. The m-th element of $\hat{\mathbf{s}}_2^{(j)}$ is the *a posteriori* mean of the corresponding symbol, calculated as

$$\begin{aligned}\hat{s}_{i_{D+m}}^{(j)} &= \textstyle\sum_{k=1}^{Q}\chi_k P\left(s_{i_{D+m}}=\chi_k|\mathbf{y}_j\right),\\ &\text{for}\quad m=1,2,\cdots,M,\end{aligned} \tag{6}$$

where $\chi_k\in\mathcal{S}$ is a Q-ary modulation symbol, and $P\left(s_{i_{D+m}}=\chi_k|\mathbf{y}_j\right)$ is the *a posteriori* probability (APP) at the output of the j-th BDFE. The adoption of the *a posteriori* soft decision reduces the effects of error propagation, which leads to better performance than hard decisions.

To compute (6), we note that the output of the feedfoward filter, denoted as $\mathbf{r}_j=[r_1^{(j)},\cdots,r_M^{(j)}]^T$, can be computed from (5) as

$$\mathbf{r}_j=\mathbf{W}\mathbf{y}_j=\mathbf{G}\mathbf{s}_2^{(j)}+\mathbf{e}_j, \tag{7}$$

where $\mathbf{G}=\mathbf{B}+\mathbf{I}_M$ is the equivalent channel matrix, and $\mathbf{e}_j=[e_1^{(j)},\cdots,e_M^{(j)}]^T$ is the noise sample vector of the equivalent system $\mathbf{G}$. The equivalent noise vector $\mathbf{e}_j$ has zero mean, and its covariance matrix is $\mathbf{\Phi}_{ee}=\mathbf{\Delta}^{-1}=\text{Diag}[\sigma_1^2,\cdots,\sigma_M^2]$, where $1/\sigma_m^2$ is the m-th diagonal element of $\mathbf{\Delta}$. Based on the assumption that $\mathbf{e}_j$ is complex Gaussian distributed, we have

$$P\left(s_{i_{D+m}}|\mathbf{r}_j\right)=\frac{P(\chi_k)}{A_m}\exp\left[-\frac{1}{\sigma_m^2}\left|\rho_m^{(j)}(s_{i_{D+m}})\right|^2\right] \tag{8}$$

where $P(\chi_k)=1/Q$ for the first iteration, A_m is a normalization constant, and the metric $\rho_m^{(j)}(s_{i_{D+m}})$ is calculated as

$$\rho_m^{(j)}(s_{i_{D+m}})=r_m^{(j)}-g_{m,m}s_{i_{D+m}}-\sum_{l=m+1}^{M}g_{m,l}\hat{s}_{i_{D+l}}^{(j)}, \tag{9}$$

where $g_{m,n}$ is the (m,n)-th element of $\mathbf{G}$.

The APP in (8) is used to replace $P\left(s_{i_{D+m}}=\chi_k|\mathbf{y}_j\right)$ in (6) for computing the soft decisions. Once the tentative soft decision vectors $\left\{\hat{\mathbf{s}}_2^{(j)}\right\}_{j=1}^{J}$ are obtained for all J parallel subsystems, they are combined with the corresponding $\mathbf{s}_1^{(j)}$ to yield J candidate estimates of the transmitted $\mathbf{s}$. The minimum Euclidean distance (MED) rule is then used to choose the best estimate out of the J candidates as

$$j_0=\arg\min_{j\in\mathcal{J}}\|\mathbf{y}-\mathbf{H}_1\mathbf{s}_1^{(j)}-\mathbf{H}_2\hat{\mathbf{s}}_2^{(j)}\|^2, \tag{10}$$

where $\mathcal{J}$ is the candidate set of the index j. The solution to (10) yields $\hat{\mathbf{s}}^{(j_0)}=\left[\mathbf{s}_1^{(j_0)};\hat{\mathbf{s}}_2^{(j_0)}\right]\in\mathcal{C}^{N\times 1}$, where $[\mathbf{a};\mathbf{b}]$ denotes the operator that stacks the two column vectors $\mathbf{a}$ and $\mathbf{b}$ into a single column vector. In the vector $\hat{\mathbf{s}}^{(j_0)}$, the first D elements are hard decisions, and the last M symbols are soft decisions. The APP of $\hat{\mathbf{s}}_2^{(j_0)}$ has been calculated in (8). The APP for the n-th symbol in $\mathbf{s}_1^{(j_0)}$ can be calculated as

$$\begin{aligned}P(s_{i_n}|\mathbf{y}) &= \tfrac{P(s_{i_n})}{A_{i_n}}\exp\left[-\tfrac{1}{\sigma_0^2}\|\mathbf{y}-\mathbf{H}\hat{\mathbf{s}}_{i_n}^{(j_0)}-\mathbf{h}_{i_n}s_{i_n}\|^2\right],\\ &\qquad i_n=i_1\cdots i_D,\end{aligned} \tag{11}$$

where $\hat{\mathbf{s}}_{i_n}^{(j_0)}$ is obtained by replacing the n-th element of $\hat{\mathbf{s}}^{(j_0)}$ with zero. The extrinsic bit LLR can then be calculated from the symbol APP as in [22], and it is used as the *a priori* LLR at the input of the channel decoder .

The selection of the candidate index set $\mathcal{J}$ is critical to the complexity-performance tradeoff of the proposed scheme. We now propose a new algorithm to reduce the size of the candidate set $\mathcal{J}$ while keeping the probability of missing the true sequence low. During the first iteration, there is no *a priori* information available. We thus propose to use the norm of the output of the feedforward filter, $\|\mathbf{r}_j\|^2$, as a metric for the candidate set selection. That is, if $M_l\le\|\mathbf{r}_j\|^2\le M_u$, where the lower and upper bounds M_l and M_u are dynamically calculated based on the channel condition, then $j\in\mathcal{J}$, otherwise $j\notin\mathcal{J}$. The bounds M_l and M_u are calculated to ensure that the true sequence is in $\mathcal{J}$ with a high probability. Therefore, the calculation of M_l and M_u requires the statistical properties of $\|\mathbf{r}_j\|^2=\sum_{m=1}^{M}|r_m^{(j)}|^2$, where $r_m^{(j)}$ is the m-th element of the vector $\mathbf{r}_j$.

Conditioned on the upper triangular equivalent channel matrix $\mathbf{G}$ and the actual transmitted sequence $\mathbf{s}^{(j)}=\mathbf{s}$, $|r_m^{(j)}|^2$ can be approximated by a non-central Chi-squared random variable with two degrees of freedom. Denote the random variable as X_m. The conditional CDF of X_m can be expressed as [26]

$$F_{X_m}(x_m|\mathbf{s},\mathbf{G})=1-Q_1\left(\frac{\sqrt{E_m}}{\sigma_m},\frac{\sqrt{x_m}}{\sigma_m}\right), \tag{12}$$

where $E_m\triangleq|\mathbf{g}_m\mathbf{s}_2|^2=|\sum_{l=m}^{M}g_{m,l}s_{i_{D+l}}|^2$, and $\mathbf{g}_m$ is the m-th row of the matrix $\mathbf{G}$. The function $Q_1(a,b)$ is the marcum-Q function with order one, defined as

$$Q_1(a,b)=\int_b^\infty x\exp\left(-\frac{x^2+a^2}{2}\right)I_0(ax)dx, \tag{13}$$

where $I_0(x)$ is the modified Bessel function of the first kind with order zero.

The probability that X_m falls between the interval $[R_m^{(l)},R_m^{(u)}]$ is

$$P(R_m^{(l)}<X_m\le R_m^{(u)})=F_{X_m}(R_m^{(u)}|\mathbf{s},\mathbf{G})-F_{X_m}(R_m^{(l)}|\mathbf{s},\mathbf{G}). \tag{14}$$

Denote

$$F_{X_m}(R_m^{(l)}|\mathbf{s},\mathbf{G})=k_l, \tag{15a}$$

$$F_{X_m}(R_m^{(u)}|\mathbf{s},\mathbf{G})=k_u, \tag{15b}$$

where $0\le k_l<k_u\le 1$. To ensure that the transmitted sequence falls in the set $\mathcal{J}$ with a high probability, k_l is chosen to be close to zero while k_u is close to one. For example, $k_l=0.01$ and $k_u=0.99$ yields a probability of

0018-9545 (c) 2013 IEEE. Personal use is permitted, but republication/redistribution requires IEEE permission. See http://www.ieee.org/publications_standards/publications/rights/index.html for more information.

This article has been accepted for publication in a future issue of this journal, but has not been fully edited. Content may change prior to final publication. Citation information: DOI 10.1109/TVT.2014.2298232, IEEE Transactions on Vehicular Technology

$k_u - k_l = 0.98$. Given k_l, k_u, and E_m, the values $R_m^{(l)}$ and $R_m^{(u)}$ can be calculated from (12) and (15). However, the value of E_m depends on the transmitted vector $\mathbf{x}$, which is not available at the receiver before detection. We propose to solve this problem by using an approximated upper bound and lower bound of E_m. The approximated upper bound is

$$\begin{aligned} E_m &\leq \sum_{l=m}^{M} |g_{m,l}|^2 \sum_{l=m}^{M} |s_{i_{D+l}}|^2 \\ &\approx (M-m+1)E_0 \|\mathbf{g}_m\|^2 \triangleq E_m^{(u)}, \end{aligned} \tag{16}$$

where $E_0 = E[|s_{D+l}|^2]$ is used to approximate $|s_{i_{D+l}}|^2$.

The lower bound of E_m is estimated as

$$E_m \geq E_0 \triangleq E_m^{(l)}. \tag{17}$$

by noting that $g_{m,m} = 1$.

The values of $R_m^{(l)}$ and $R_m^{(u)}$ can then be solved from (15) by using $E_m^{(u)}$ and $E_m^{(l)}$, respectively. Once $R_m^{(l)}$ and $R_m^{(u)}$ are calculated, the overall upper and lower bounds of $||\mathbf{r}_j||^2$ can be obtained as

$$M_u = \sum_{m=1}^{M} R_m^{(u)}, \tag{18}$$

$$M_l = \sum_{m=1}^{M} R_m^{(l)}. \tag{19}$$

The approximation in (16) can achieve a good performance for constant-modulus modulation schemes, such as phase shift keying, because all the symbols have the same average power E_0. On the other hand, for modulation schemes with non-constant amplitude, some performance loss may occur. In this case, the maximum symbol energy $E_{\max}$ can be used to replace E_0 in $E_m^{(u)}$, and the minimum symbol energy $E_{\min}$ is used to replace E_0 in $E_m^{(l)}$. Such a mechanism can achieve good performance with a slightly higher complexity.

The candidate set $\mathcal{J}$ in the first iteration is constructed by choosing sequences with $\|\mathbf{r}_j\|^2 \in [M_l, M_u]$ as its members. Such a scheme yields a set with cardinality far less than Q^D; thus the complexity is reduced significantly compared to GPIC, which exhaustively searches over all the Q^D possible sequences of $\mathbf{s}_1$. At the mean time, the calculation of M_u and M_l ensures that the transmitted sequence will fall in $\mathcal{J}$ with a high probability. During the first iteration, the same feedforward filter is used for all the subsystems and the bound calculation. The evaluation of the Marcum-Q function can be performed by using a look-up table to reduce the complexity.

The first iteration of the proposed S-PIC-BDFE scheme is summarized in Table I.

B. Second Iteration and Beyond

Since the *a priori* information is available for the second iteration and beyond, the candidate set for $\mathbf{s}_1$ is updated based on the *a priori* LLR $L_{A1}^{n,p}$ at the input of the UD-MIMO detector. The *a priori* probability for coded bits $c_{n,p}$ is calculated as

$$\begin{aligned} P(c_{n,p}=0) &= \frac{\exp(L_{A1}^{n,p})}{1+\exp(L_{A1}^{n,p})}, \\ P(c_{n,p}=1) &= \frac{1}{1+\exp(L_{A1}^{n,p})}. \end{aligned} \tag{20}$$

Assume that the constellation symbol χ_k is mapped to the bit pattern $[b_{k,1}, \cdots, b_{k,P}]^T$, then the symbol probability $P(s_n = \chi_k)$ is calculated from (20) as

$$\log P(s_n = \chi_k) = \textstyle\sum_{i=1}^{P} \log P(c_{n,p} = b_{k,i}), \quad \text{for} \quad k = 1, \cdots, Q. \tag{21}$$

Let a possible transmitted symbol sequence of subsystem $\mathbf{H}_1$ be $\mathbf{s}_1^{(j)} = [s_{i_1}^{(j)}, \cdots, s_{i_D}^{(j)}]^T$, and all elements of $\mathbf{s}_1^{(j)}$ are independent. Then the probability of $\mathbf{s}_1 = \mathbf{s}_1^{(j)}$ can be calculated from (21) as

$$\log P(\mathbf{s}_1 = \mathbf{s}_1^{(j)}) = \textstyle\sum_{d=1}^{D} \log P(s_d = s_{i_d}^{(j)}), \quad \text{for} \quad j = 1, \cdots, Q^D. \tag{22}$$

Ideally, we can calculate all Q^D probabilities in (22) and select the sequences with the highest probabilities as the candidate set. However, this involves exhaustive search of Q^D probabilities, thus leading to high computational complexity. To further reduce complexity, we propose a per-antenna selection approach by reducing the number of candidate symbols on each antenna. That is, the *a priori* symbol probabilities calculated from (21) for antenna n are sorted in a descending order, and the K symbols with the highest probabilities are chosen as the candidate symbols. Only the K candidate symbols on each antenna are used for the calculation of the sequence *a priori* probability in (22), which yields $J = K^D$ candidate sequences. The value of $K \in [1, Q]$ can be chosen to balance the complexity-performance tradeoff.

After the candidate set is selected, the PIC in (4) is used again to yield J parallel symmetric subsystems. Then the BDFE algorithm is used to detect the J sequences $\mathbf{s}_2^{(j)}$ in parallel. Since the *a priori* information is available from the previous iteration, the inputs to the BDFE filters, as well as the filter coefficients, are different from those in the first iteration. With the aid of the *a priori* LLR $L_{A1}^{n,p}$, the *a priori* mean and variance of the symbol at the i_{D+m}-th antenna is calculated as

$$\begin{aligned} \bar{s}_{i_{D+m}} &= \sum_{k=1}^{Q} \chi_k P(s_{i_{D+m}} = \chi_k), \\ \sigma_{i_{D+m}}^2 &= \sum_{k=1}^{Q} |\chi_k - \bar{s}_{i_{D+m}}|^2 P(s_{i_{D+m}} = \chi_k), \end{aligned} \tag{23}$$

where $m = 1, \cdots, M$, and $P(s_{i_{D+m}} = \chi_k)$ is obtained from (20) and (21).

For the j-th symmetric subsystem, the BDFE filter matrices for the detection of the $(D+m)$-th symbol are

$$\begin{aligned} \mathbf{B}_m &= \mathbf{U}_m - \mathbf{I}_M, \\ \mathbf{W}_m &= \mathbf{U}_m \mathbf{\Phi}_m \mathbf{H}_2^H \left(\mathbf{H}_2 \mathbf{\Phi}_m \mathbf{H}_2^H + \sigma_0^2 \mathbf{I}_M\right)^{-1}, \end{aligned} \tag{24}$$

where $\mathbf{\Phi}_m$ is the *a priori* covariance matrix for the equalization

0018-9545 (c) 2013 IEEE. Personal use is permitted, but republication/redistribution requires IEEE permission. See http://www.ieee.org/publications_standards/publications/rights/index.html for more information.

This article has been accepted for publication in a future issue of this journal, but has not been fully edited. Content may change prior to final publication. Citation information: DOI 10.1109/TVT.2014.2298232, IEEE Transactions on Vehicular Technology

TABLE I
THE S-PIC-BDFE ALGORITHM FOR THE FIRST ITERATION

Parameters	thresholds $0 \le k_l < k_u \le 1$, constellation symbols χ_k for $k = 1, \cdots, Q$.
Inputs	the channel matrix $\mathbf{H}$, noise variance σ_0^2, and the received signal $\mathbf{y}$
Step 1	Channel ordering and partitioning
1.1	compute the Frobenius norms $\|\|(\mathbf{H}^\dagger)_k\|\|$;
1.2	order the norms in an ascending order to yield the ordered index set $\{i_n\}_{n=1}^N$;
1.3	partition $\mathbf{H}_1 = [\mathbf{h}_{i_1}, \cdots, \mathbf{h}_{i_D}]$ and $\mathbf{H}_2 = [\mathbf{h}_{i_{D+1}}, \cdots, \mathbf{h}_{i_N}]$;
Step 2	BDFE filter design
2.1	compute filters $\mathbf{B}$ and $\mathbf{W}$ as in (5). Set $\mathbf{G} = \mathbf{B} + \mathbf{I}_M$;
2.2	compute column vector norms $\|\|\mathbf{g}_m\|\|^2$ for $m = 1, \cdots, M$.
Step 3	Bounds calculations for $\|\|\mathbf{r}_j\|\|^2$
3.1	compute $E_m^{(u)}$ and $E_m^{(l)}$ with (16) and (17), respectively;
3.2	compute $R_m^{(u)}$ and $R_m^{(l)}$ by (15a) and (15b), respectively;
3.3	compute M_u and M_l by (18) and (19), respectively;
Step 4	PIC and BDFE detection
4.1	for each $\mathbf{s}_1^{(j)}$, compute $\mathbf{s}_2^{(j)}$ and $\mathbf{r}_j$ according to (4) and (7), and compute the norm of $\mathbf{r}_j$;
4.2	if $M_l \le \|\|\mathbf{r}_j\|\|^2 \le M_u$, then choose the j and go to Step 4.3, otherwise return to Step 4.1;
4.3	for $j \in \mathcal{J}$, compute the APP by (8) and (9); then compute the soft decision for $\hat{\mathbf{s}}_2^{(j)}$ by (6);
Step 5	j_0 selection and APP calculation
5.1	compute MED according to (10) for each $j \in \mathcal{J}$;
5.2	find j_0 with the minimum MED;
5.3	compute the APP for $\mathbf{s}_1^{(j_0)}$ by (11).

of $s_{i_{D+m}}^{(j)}$, and it is

$$\mathbf{\Phi}_m = \text{Diag}\{\sigma_{i_{D+1}}^2, \cdots, \sigma_{i_{D+m-1}}^2, 1, \sigma_{i_{D+m+1}}^2, \cdots, \sigma_{i_N}^2\}.$$

The matrix $\mathbf{U}_m$ is calculated from the Cholesky decomposition

$$\frac{1}{E_s}\mathbf{\Phi}_m^{-1} + \frac{1}{\sigma_0^2}\mathbf{H}_2^H\mathbf{H}_2 = \mathbf{U}_m^H\mathbf{\Delta}\mathbf{U}_m.$$

which is also related to $\mathbf{\Phi}_m$. It is noted that, although the filter matrices $\mathbf{B}_m$ and $\mathbf{W}_m$ are different for each m, they are the same for all j, since the variance calculated from (23) is the same for all the J parallel subsystems.

The output of the j-th subsystem is

$$\mathbf{r}_m^{(j)} = \mathbf{W}_m(\mathbf{y}_j - \mathbf{H}_2\bar{\mathbf{s}}_{2m}) = \mathbf{G}_m(\mathbf{s}_2^{(j)} - \bar{\mathbf{s}}_{2m}) + \mathbf{e}_m^{(j)}, \quad (25)$$

where $\mathbf{e}_m^{(j)}$ is the error vector of the equivalent system $\mathbf{G}_m = \mathbf{B}_m + \mathbf{I}_M$, and $\bar{\mathbf{s}}_{2m}$ is the *a priori* mean vector with the m-th element being zero. That is

$$\bar{\mathbf{s}}_{2m} = [\bar{s}_{i_{D+1}}, \cdots, \bar{s}_{i_{D+m-1}}, 0, \bar{s}_{i_{D+m+1}}, \cdots, \bar{s}_{i_N}]^T,$$

which is the same for all j since the mean calculated from (23) is the same for all the J parallel subsystems. The soft decision at the output of the BDFE filter can then be calculated in a similar manner as (6) and (8).

From (25) it is observed that the equivalent system for the second iteration and beyond is more complicated than that of the first iteration. During the APP calculation in (8) for the second or later iterations, the metric $\rho_m^{(j)}(s_{i_{D+m}})$ is calculated as

$$\begin{aligned}\rho_m^{(j)}(s_{i_{D+m}}) &= r_m^{(m,j)} - g_{m,m}s_{i_{D+m}} \\ &- \sum_{l=m+1}^{M} g_{m,l}(\hat{s}_{i_{D+l}}^{(j)} - \bar{s}_{i_{D+l}}), \end{aligned} \quad (26)$$

where $r_m^{(m,j)}$ is the m-th element of $\mathbf{r}_m^{(j)}$ and $\hat{s}_i^{(j)}$ is the i-th soft decision of the j-th subsystem of the current iteration.

The UD-MIMO detection algorithm for the second iteration and beyond is summarized in Table II.

IV. COMPLEXITY ANALYSIS

In this section, the complexity of the proposed S-PIC-BDFE scheme is analyzed and compared to that of the conventional GPIC-GSIC-BDFE scheme [23]. Several steps are common to both algorithms, such as channel ordering and partition, and LLR calculation in the channel decoder. The channel ordering and partition are performed only once and its complexity is relatively low; thus we omit them in the analysis. The complexity of the LLR calculation is also small compared to the other steps, especially if we use the MAX-log-MAP approximation; thus it is also ignored in our analysis. Hence, the complexity analysis focuses on the number of complex multiplications in the symbol detection part of the algorithms.

For the first iteration, since the BDFE filter matrices $\mathbf{W}$ and $\mathbf{B}$ are the same for all the J parallel subsystems and all symbols, they are calculated only once and the complexity is

0018-9545 (c) 2013 IEEE. Personal use is permitted, but republication/redistribution requires IEEE permission. See http://www.ieee.org/publications_standards/publications/rights/index.html for more information.

This article has been accepted for publication in a future issue of this journal, but has not been fully edited. Content may change prior to final publication. Citation information: DOI 10.1109/TVT.2014.2298232, IEEE Transactions on Vehicular Technology

TABLE II
THE S-PIC-BDFE ALGORITHM FOR THE SECOND ITERATION AND BEYOND

Parameters	number of candidates per transmit antenna $K < Q$, constellation symbols χ_k for $k = 1, \cdots, Q$.
Inputs	LLR $L_{A1}^{n,p}$, channel partition $[\mathbf{H}_1, \mathbf{H}_2]$, noise variance σ_0^2, and the received signal $\mathbf{y}$
Step 1	Candidate set selection
1.1	compute the *a priori* probability for each symbol $s_{i_d} = \chi_k$, for $d = 1 : D$ and $k = 1 : Q$
1.2	for each d, pick the K symbols with the largest *a priori* probabilities
1.3	form the candidate set with the $J = K^D$ selected symbols
Step 2	BDFE filter design
2.1	compute symbol mean and variance from the LLR input by (23)
2.2	compute variance matrix $\mathbf{\Phi}_m$ and upper triangular matrix $\mathbf{U}_m$
2.3	compute filters $\mathbf{B}_m$ and $\mathbf{W}_m$ as in (24). Set $\mathbf{G}_m = \mathbf{B}_m + \mathbf{I}_M$;
Step 3	PIC and BDFE detection
3.1	for $j = 1 : J$, compute $\mathbf{y}_j$ by (4) and $\mathbf{r}_j$ by (25),
3.2	compute the APP by (8) and (26);
3.3	compute the soft decision for $\mathbf{s}_2^{(j)}$ by (6);
Step 4	j_0 selection and APP calculation — the same as Step 5 of the first iteration in Table I.

negligible. Thus their complexity are not taken into account. For the proposed algorithm, the average number of complex multiplications can be written as

$$N_{CM} = JN_{sys} + N_{bound} + N_{norm}, \tag{27}$$

where J denotes the size of the candidate set, N_{sys} denotes the number of complex multiplications of detecting a subsystem, N_{bound} contains the operations used for the calculation of the bounds of $\|\mathbf{r}_j\|^2$ during the first iteration, and N_{norm} contains the calculation of $||\mathbf{r}_j||^2$ for all the subsystems. The average number of complex multiplications incurred by the calculation of $||\mathbf{r}_j||^2 = ||\mathbf{W}(\mathbf{y} - \mathbf{H}_1\mathbf{s}_1^{(j)})||^2$ is $N_{norm} = Q^D(DM + M^2)$.

The computation of the bounds of $||\mathbf{r}_j||^2$ involves three operations, the calculation of the CDF in (12), the calculation of the bounds in (18) and (19), and the norm calculation in (16). The CDF calculation can be performed with a two-dimensional lookup table, and the actual bounds calculations in (18) and (19) require only a small amount of multiplications. These two operations involve only negligible amount of complexity. Thus the complexity is mainly contributed by the norm calculation. Since $\mathbf{G}$ is upper-triangular, $N_{bounds} = \frac{M^2+M}{2}$.

The number of complex multiplications of detecting a subsystem, N_{sys}, is obtained as follows. Only the feedback filter is used in the detection for each subsystem. With (8) and (9), and considering the upper-triangular structure of the matrix $\mathbf{G}$, $(M - m + 1)Q$ complex multiplications are required for the calculation of the component $s_{i_{D+m}}$. In order to obtain the *a posteriori* probability in (8), three real multiplications are required and they are counted as one complex multiplication. The Euclidean distance calculation in (10) incurs M^2 complex multiplications. Therefore, the detection of one subsystem requires $\sum_{m=1}^{M}(M - m + 2)Q + M^2 = \frac{M(M+3)}{2}Q + M^2$ complex multiplications.

Based on the above analysis, (27) can be written as

$$\begin{aligned} N_{CM} &\simeq J\left(\frac{M(M+3)}{2}Q + M^2\right) + Q^D(DM + M^2) \\ &+ \frac{M^2 + M}{2}. \end{aligned} \tag{28}$$

The parameter J can be estimated by counting the number of $\mathbf{s}_1^{(j)}$ that satisfy

$$r_1^2 \le ||\mathbf{r}_j||^2 \le r_2^2, \tag{29}$$

where $r_1 = \sqrt{M_l}$, $r_2 = \sqrt{M_u}$ are the bounds computed according to Table I. Eqn. (29) can be alternatively expressed as

$$r_1^2 \le ||\mathbf{y}_0 - \mathbf{H}_0\mathbf{s}_1^{(j)}||^2 \le r_2^2. \tag{30}$$

where $\mathbf{y}_0 = \mathbf{W}\mathbf{y}$ is the output of the feedforward filter, and $\mathbf{H}_0 = \mathbf{W}\mathbf{H}_1$ is the equivalent channel matrix after the feedforward filter.

The value of J can thus be identified by finding the number of vectors $\mathbf{s}_1^{(j)}$ that lie within the hyper spherical shell defined by (30). According to [27], for an infinite set, the number of vectors that lie within a hyper-sphere with radius r can be approximated by

$$J_r \simeq \frac{V_r}{V_{basis}}, \tag{31}$$

where V_r is the volume of a hyper-sphere with radius r, and V_{basis} is the volume of the fundamental region of the set under consideration. For a complex set with order M, the volume of a hyper-sphere with radius r is

$$V_r = \frac{\pi^M r^{2M}}{M!}. \tag{32}$$

The volume of the fundamental region of a real-valued set

0018-9545 (c) 2013 IEEE. Personal use is permitted, but republication/redistribution requires IEEE permission. See http://www.ieee.org/publications_standards/publications/rights/index.html for more information.

This article has been accepted for publication in a future issue of this journal, but has not been fully edited. Content may change prior to final publication. Citation information: DOI 10.1109/TVT.2014.2298232, IEEE Transactions on Vehicular Technology

is [28]

$$V_{basis} = \sqrt{\det(\mathbf{\Lambda}^T \mathbf{\Lambda})}, \tag{33}$$

where the column vectors of the matrix $\mathbf{\Lambda}$ form the bases of the set. Since the equivalent channel matrix $\mathbf{H}_0$ is of complex-valued, we convert it into an equivalent real-valued representation

$$\begin{bmatrix} \mathcal{R}\left(\mathbf{H}_0 \mathbf{s}_1^{(j)}\right) \\ \mathcal{I}\left(\mathbf{H}_0 \mathbf{s}_1^{(j)}\right) \end{bmatrix} = \begin{bmatrix} \mathcal{R}(\mathbf{H}_0) & -\mathcal{I}(\mathbf{H}_0) \\ \mathcal{I}(\mathbf{H}_0) & \mathcal{R}(\mathbf{H}_0) \end{bmatrix} \begin{bmatrix} \mathcal{R}(\mathbf{s}_1^{(j)}) \\ \mathcal{I}(\mathbf{s}_1^{(j)}) \end{bmatrix}. \tag{34}$$

Define $\tilde{\mathbf{H}}_0 = \begin{bmatrix} \mathcal{R}(\mathbf{H}_0) & -\mathcal{I}(\mathbf{H}_0) \\ \mathcal{I}(\mathbf{H}_0) & \mathcal{R}(\mathbf{H}_0) \end{bmatrix}$. If $D \leq M$, the matrix $\tilde{\mathbf{G}} = \tilde{\mathbf{H}}_0^T \tilde{\mathbf{H}}_0$ is of full-rank. Thus we can directly use $\mathbf{\Lambda} = \tilde{\mathbf{H}}_0$ in (33).

If $D > M$, the matrix $\tilde{\mathbf{H}}_0^T \tilde{\mathbf{H}}_0$ is a rank-deficient matrix, which cannot be used to describe the property of the fundamental region. In this case, we let $\mathbf{\Lambda} = \tilde{\mathbf{H}}_0^T$ in (33). Since the transmit vector is normalized to unit energy, a normalization factor α should be used, and the volume of the fundamental region is then computed as

$$V_{basis} = \alpha \sqrt{\det(\tilde{\mathbf{H}}_0 \tilde{\mathbf{H}}_0^T)}. \tag{35}$$

For example, $\alpha = 0.2673$ for quadrature phase shift keying (QPSK) modulation and $\alpha = 0.1195$ for sixteen quadrature amplitude modulation (16QAM).

Combining (32) and (35) yields an estimate of J

$$\hat{J} = \frac{V_{r_2} - V_{r_1}}{V_{basis}} = \frac{1}{\alpha\beta} \frac{\pi^M (r_2^{2M} - r_1^{2M})}{M! \sqrt{\det(\tilde{\mathbf{H}}_0 \tilde{\mathbf{H}}_0^T)}}. \tag{36}$$

where β is an adjustment factor used to account for the fact that the vectors are from a finite set instead of an infinite set. It should be noted that the method of complexity analysis in this section is suitable only for lattice-based modulation. Substituting (36) into (28) leads to an estimate of the number of complex multiplications of the proposed algorithm in the first iteration.

For the conventional GPIC-BDFE scheme, an exhaustive search over the Q^D dimensional signal space is required and the number of the subsystems is always Q^D. In addition, the calculation of the bounds are not required for the GPIC-BDFE scheme. Substituting J with Q^D in (28) and removing the last term, we can obtain the number of the complex multiplications of the GPIC-BDFE scheme.

For the second iteration and beyond, even though the coefficient matrices $\mathbf{W}_m$ and $\mathbf{B}_m$ are still the same for all the subsystems, they change with respect to the receive antenna index m. Therefore, M pairs of $\mathbf{W}_m$ and $\mathbf{B}_m$ should be calculated and this incurs a complexity on the order of $\mathcal{O}\left(\frac{3}{2}M^4\right)$. For each subsystem, the BDFE algorithm requires $2M$ matrix multiplications between a $(M \times M)$ matrix and a $(M \times 1)$ vector, and the complexity is on the order of $\mathcal{O}\left(M^3\right)$. Thus the overall complexity is on the order of $\mathcal{O}\left(\frac{3}{2}M^4 + K^D M^3\right)$ with $K \leq Q$. For the GPIC-GSIC-BDFE scheme [23], the number of subsystems is $\lceil \frac{N}{M} \rceil$ in the GSIC step, and the overall complexity is approximately $\mathcal{O}\left(\frac{3}{2}NM^3\right)$.

The complexity of the second and later iterations of the proposed scheme is mainly determined by D. For a large D, the proposed scheme has a higher complexity but better performance than the GPIC-GSIC-BDFE scheme. However the overall complexity is mainly determined by the complexity of the first iteration. The proposed algorithm reduces the complexity of the first iteration significantly. It is shown through numerical analysis that, compared to the GPIC-GSIC-BDFE scheme, the proposed scheme can simultaneously reduce the overall complexity and improve the overall performance.

V. Simulation Results

In this section, the performance of the proposed S-PIC-BDFE scheme is evaluated. The simulation results of a 7×3 UD-MIMO system are illustrated first. At the transmitter, a rate $1/2$ systematic convolutional code with the generator polynomial $G = [7, 5]_8$ is employed. Modulation schemes include QPSK, eight PSK (8PSK) and 16QAM. With full multiplexing gain, the UD-MIMO system can achieve a spectral efficiency of 14, 21, and 28 bits/s/Hz for QPSK, 8PSK, and 16QAM, respectively. The channel is assumed to be frequency-flat Rayleigh fading. The S-PIC-BDFE algorithm is applied at the receiver. For the first iteration, we choose $k_l = 0.01$ and $k_u = 0.99$ for bound calculation. Since the total average transmit energy across all N antennas is normalized to $E_s = 1$, the average symbol energy is $E_0 = E_s/N = 1/7$. For 16QAM, the minimum symbol energy $E_{\min} = 0.2/7$ is used to replace E_0 when estimating the minimum value of $E_m^{(l)}$. For the second iteration and beyond, we choose $K = 2$ for the candidate set selection, and this yields $J = K^D = 16$ parallel subsystems.

The BER performances of the proposed S-PIC-BDFE algorithm are shown in Figure 3, and they are compared to those of the GPIC-GSIC-BDFE algorithm [23]. During the first iteration, the performance of the S-PIC-BDFE is almost identical to the GPIC-BDFE, even though the number of subsystems explored by the S-PIC-BDFE is much less than that of the GPIC-GSIC-BDFE that performs exhaustive search over all the possible Q^D subsystems. For the second and later iterations, the S-PIC-BDFE outperforms its GPIC-GSIC-BDFE counterparts, and the performance difference becomes more pronounced for systems with larger constellation sizes. For example, at BER = 10^{-3} and during the fifth iteration, the S-PIC-BDFE achieves a 0.6 dB and 0.8 dB performance gain over the GPIC-GSIC-BDFE scheme for systems with 8PSK and 16QAM, respectively.

The performance of the proposed S-PIC-BDFE algorithm depends heavily on the construction of the candidate set. Figure 4(a) shows the probability that the candidate set contains the transmitted $\mathbf{s}_1$ for a system with 8PSK modulation. In the first iteration, the true $\mathbf{s}_1$ is in the candidate set with a probability higher than 99.8% even at a relatively lower E_b/N_0. Such a result indicates that the proposed new candidate selection method for the first iteration can achieve a performance that is very close to the exhaustive search, and this corroborates the BER results in Fig. 3. However, the probability of including the true $\mathbf{s}_1$ drops to 92% at the second iteration at E_b/N_0 = 18 dB, and it gradually increases as the iteration progresses. In the second and later iterations, the candidate set selection is performed by using the *a priori* soft information, the reliability

0018-9545 (c) 2013 IEEE. Personal use is permitted, but republication/redistribution requires IEEE permission. See http://www.ieee.org/publications_standards/publications/rights/index.html for more information.

This article has been accepted for publication in a future issue of this journal, but has not been fully edited. Content may change prior to final publication. Citation information: DOI 10.1109/TVT.2014.2298232, IEEE Transactions on Vehicular Technology

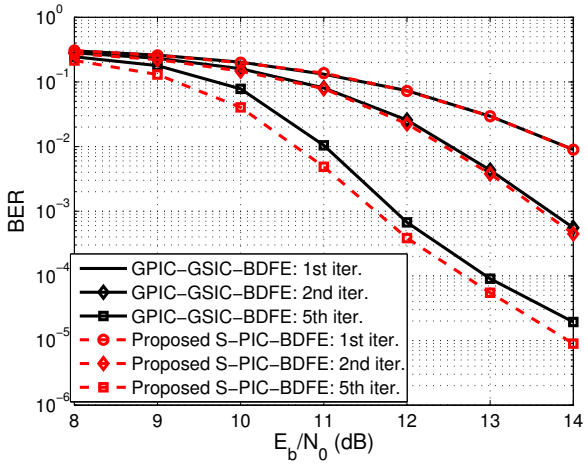

(a) QPSK

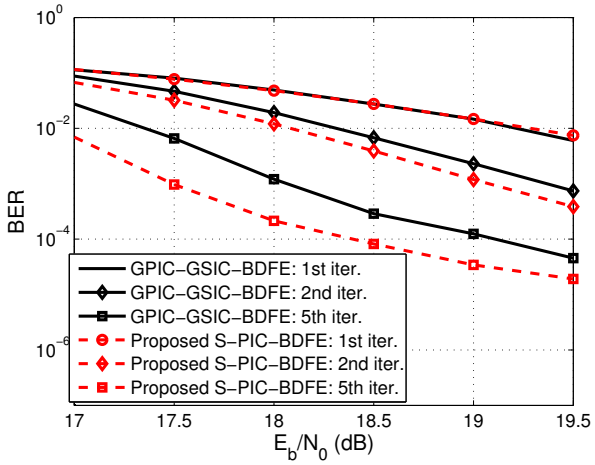

(b) 8PSK

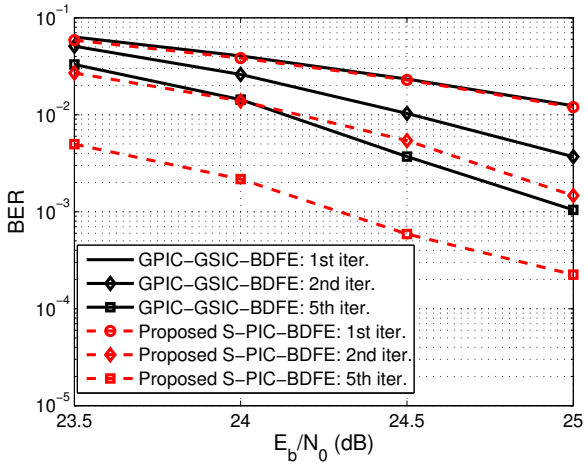

(c) 16QAM

Fig. 3. BER for 7×3 MIMO systems with flat Rayleigh fading channel.

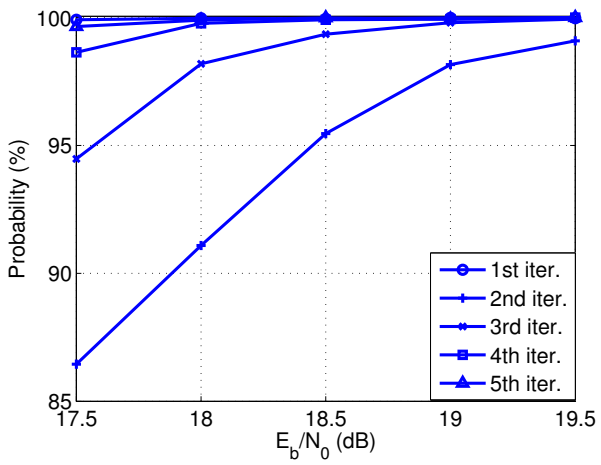

(a) Probability that the candidate set includes the true $\mathbf{s}_1$

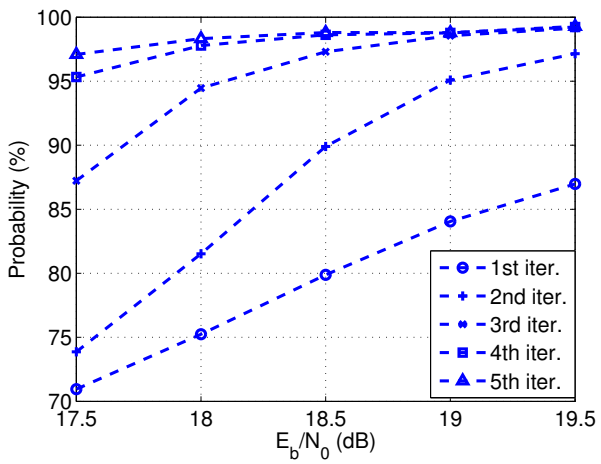

(b) Probability that the S-PIC-BDFE finds the true $\mathbf{s}_1$

Fig. 4. Probabilities of the S-PIC-BDFE algorithm with 8PSK modulation.

of which is lower at the first few iterations. At the fifth iteration, the probability of including the true $\mathbf{s}_1$ is very close to that of the first iteration.

Even though the true $\mathbf{s}_1$ is included in the candidate set, it might not be correctly detected by the BDFE and MED algorithms due to the multiplexing interference and noise. Figure 4(b) shows the probability that the true $\mathbf{s}_1$ is detected after the BDFE for the various iterations. At the first iteration, the probability of detecting the true $\mathbf{s}_1$ is relatively low because of the low detection quality of $\mathbf{s}_2$ by the BDFE algorithm. The probability increases monotonically as the iteration progresses, and it reaches over 99% at the fifth iteration at $E_b/N_o = 18.5$ dB, which corresponds to BER = 1.7×10^{-2} in Fig. 3(b). This results indicate that the simple per-antenna candidate selection method for the second iteration and beyond works very well with the S-PIC-BDFE scheme.

The parameters k_u and k_l are key to both performance and complexity. Table III shows the average number of parallel subsystems explored during the first iteration as well as the BER of the first and fifth iterations with different k_u. To simplify the analysis, we choose $k_l = 1 - k_u$. The E_b/N_0 is chosen to ensure that the UD-MIMO system achieves a relatively low BER. We choose $E_b/N_0 = 13$ dB for QPSK modulation, 18.5 dB for 8PSK, and 24 dB for 16QAM, respectively, and all yield satisfactory BER for practical systems. For the proposed algorithm, the average number of subsystems visited can be regarded as a measurement of complexity; thus Table III shows the trade-

0018-9545 (c) 2013 IEEE. Personal use is permitted, but republication/redistribution requires IEEE permission. See http://www.ieee.org/publications_standards/publications/rights/index.html for more information.

This article has been accepted for publication in a future issue of this journal, but has not been fully edited. Content may change prior to final publication. Citation information: DOI 10.1109/TVT.2014.2298232, IEEE Transactions on Vehicular Technology

TABLE III
AVERAGE NUMBER OF SUBSYSTEMS SEARCHED DURING THE FIRST ITERATION OF THE PROPOSED S-PIC-BDFE, $E_b/N_0 = 13\ dB$ FOR QPSK, $18.5\ dB$ FOR 8PSK AND $24\ dB$ FOR 16QAM

k_u	Modulation	Avg. # of subsystems	Percentage (%)	BER for 1st iter.	BER for 5th iter.
1	QPSK	238	92.97	0.0295	4.6689×10^{-5}
	8PSK	3.4×10^3	83.01	0.0273	9.7466×10^{-5}
	16QAM	3.45×10^4	52.64	0.0373	0.0013
0.99	QPSK	162	63.28	0.295	4.6689×10^{-5}
	8PSK	1.8×10^3	45.46	0.0273	9.7466×10^{-5}
	16QAM	2.48×10^4	37.84	0.0399	0.0017
0.8	QPSK	109	42.58	0.0295	5.0924×10^{-5}
	8PSK	1.4×10^3	34.18	0.0273	9.7466×10^{-5}
	16QAM	2.09×10^4	31.89	0.0426	0.0019
0.6	QPSK	90	35.16	0.0301	5.5438×10^{-5}
	8PSK	1.2×10^3	29.30	0.0274	6.5018×10^{-5}
	16QAM	2.03×10^4	30.98	0.0432	0.0020

TABLE IV
COMPARISON FOR AVERAGE NUMBER OF COMPLEX MULTIPLICATIONS DURING THE FIRST ITERATION OF THE SIMPLIFIED PIC-BDFE AND THE GPIC-BDFE

Modulation	E_b/N_0 (dB)	GPIC-BDFE	Proposed: simulated	Proposed: approximation	Percentage (%)
QPSK	13	1.69×10^4	1.29×10^4	1.34×10^4	76.33
8PSK	19	4.18×10^5	2.38×10^5	—	56.94
16QAM	24.5	1.14×10^7	5.27×10^6	5.60×10^6	46.23

off between the complexity and performance for different k_u. We observe that reducing k_u (thus increasing k_l) would reduce the average number of subsystems visited. When k_u changes from 1 to 0.99, the reduction of the average number of the subsystems is the most significant. For example, for 8PSK modulation, the average number of subsystems visited during the first iteration changes from 3.4×10^3 to 1.8×10^3. With k_u decreasing continually, the average number of subsystems also decreases, but not significantly. With appropriate choice of k_u for high order constellations, less than half of all the Q^D subsystems are explored, and this results in a more than 50% complexity reduction. The choice of k_u also affects the performance of the proposed algorithm slightly. Reducing k_u only leads to a small performance degradation. Our simulations show that, these conclusions also hold for a larger range of E_b/N_0.

Figure 5 shows the approximation of the average number of subsystems explored according to Sec. IV for the 7×3 UD-MIMO system with $k_u = 0.99$. The solid line in Fig. 5 is the actual average number of subsystems explored in the Monte Carlo simulation with 5,000 channel realizations for every E_b/N_0. From Fig. 5, we observe that $\hat{J}$ is a good approximation when the adjustment factor β is chosen as 2,048 for QPSK modulation and 512 for 16QAM modulation.

Figure 6 shows the average number of complex multiplications required for the proposed S-PIC-BDFE scheme and the GPIC-GSIC-BDFE in the first iteration with $k_u = 0.99$. Since channel ordering and the BDFE filter design are the same for both schemes, we only counted the number of complex multiplications used in the search process. Since exhaustive search is used in the first iteration of the GPIC-GSIC-BDFE scheme, the average number of multiplications of the GPIC-BDFE scheme can be also regarded as the upper bound of the complexity for the proposed S-PIC-BDFE scheme. The complexity of the proposed S-PIC-BDFE scheme is lower than that of the GPIC-BDFE for all configurations, and the difference becomes bigger at higher E_b/N_0. For QPSK modulation, the S-PIC-BDFE requires 10% to 30% less number of multiplications than the GPIC-GSIC-BDFE when the E_b/N_0 varies from 8 to 14 dB. The complexity reduction is even bigger for higher order modulations. The S-PIC-BDFE requires 40% and 60% less number of multiplications than the GPIC-GSIC-BDFE for systems with 8PSK and 16QAM, respectively. The comparison for the number of the complex multiplications is also shown in table IV. The E_b/N_0 is chosen to ensure a relatively low BER. We can observe that, for QPSK modulation, the proposed S-PIC-BDFE algorithm requires 76.33% multiplications compared with the conventional algorithm. For 8PSK and 16QAM, only 56.94% and 46.23% multiplications are required, respectively. These results indicate that the S-PIC-BDFE is more efficient for higher order modulations.

The simulation results of a 4×2 UD-MIMO system with 16QAM modulation are shown to demonstrate that the S-PIC-BDFE also works well and is efficient for other antenna configurations. The same rate $1/2$ convolutional code with the generator polynomial $G = [7, 5]_8$ was employed. The S-PIC-BDFE algorithm was applied at the receiver and the same parameters were used except that the average symbol energy

0018-9545 (c) 2013 IEEE. Personal use is permitted, but republication/redistribution requires IEEE permission. See http://www.ieee.org/publications_standards/publications/rights/index.html for more information.

This article has been accepted for publication in a future issue of this journal, but has not been fully edited. Content may change prior to final publication. Citation information: DOI 10.1109/TVT.2014.2298232, IEEE Transactions on Vehicular Technology

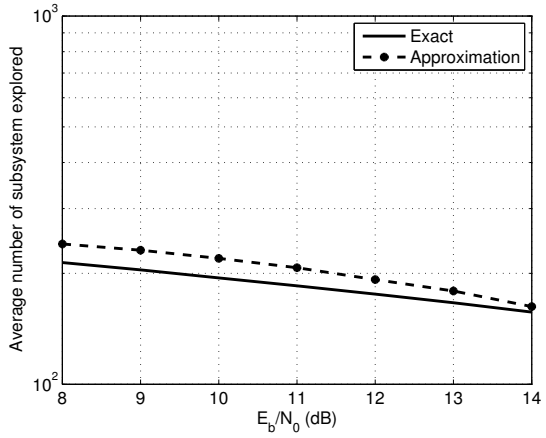

(a) QPSK

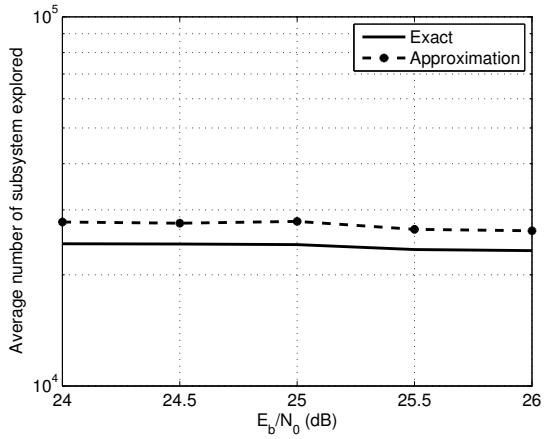

(b) 16QAM

Fig. 5. Approximation of the average number of subsystems explored for the first iteration. Parameters are $N = 7$, $M = 3$, $k_l = 0.01$ and $k_u = 0.99$. The average symbol energy $E_{mean} = 1/7$ is used to estimate the upper and lower bounds $E_m^{(u)}$ and $E_m^{(l)}$ for QPSK. The minimum symbol energy $E_{min} = 0.2/7$ is used to estimate the lower bound $E_m^{(l)}$ for 16QAM.

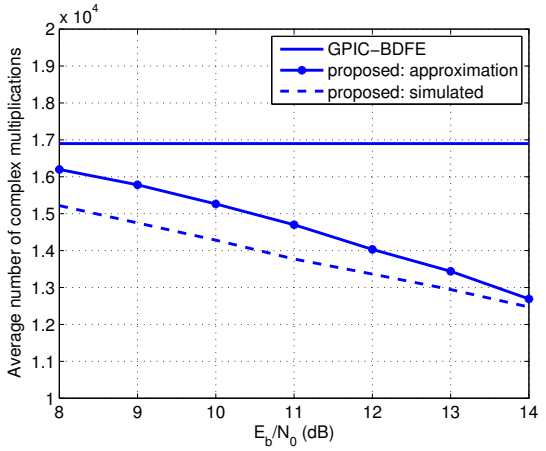

(a) QPSK

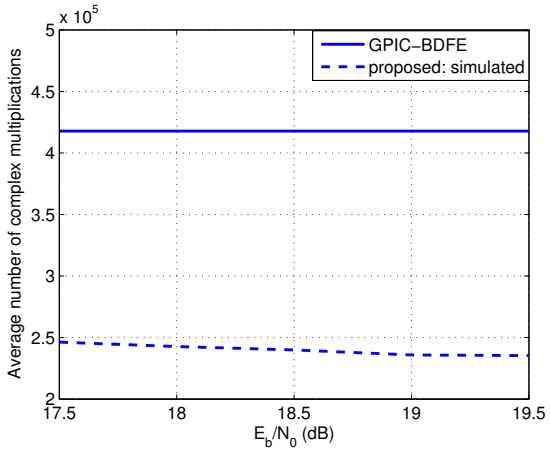

(b) 8PSK

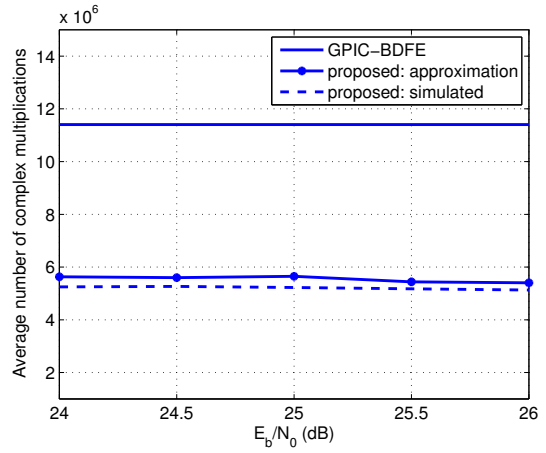

(c) 16QAM

Fig. 6. Average number of complex multiplications required for the UD-MIMO system with $N = 7$ and $M = 3$. Parameters are $k_l = 0.01$ and $k_u = 0.99$. The average symbol energy $E_{mean} = 1/7$ is used to estimate the upper and lower bounds $E_m^{(u)}$ and $E_m^{(l)}$ for QPSK and 8PSK. The minimum symbol energy $E_{min} = 0.2/7$ is used to estimate the lower bound $E_m^{(l)}$ for 16QAM.

became $E_0 = 1/4$ and the minimum symbol energy was $E_{min} = 0.2/4$.

Figure 7(a) shows the BER performance of the S-PIC-BDFE and the conventional GPIC-GSIC-BDFE. Similar to the 7×3 UD-MIMO system, the S-PIC-BDFE algorithm has the same performance as the conventional GPIC-BDFE algorithm at the first iteration and outperforms the conventional algorithm at subsequent iterations. For example, at the fifth iteration, the performance of S-PIC-BDFE algorithm is about 0.8 dB better than that of GPIC-BDFE algorithm at BER = 10^{-3}.

Figure 7(b) shows average number of complex multiplications for the 4×2 UD-MIMO with 16QAM modulation. The approximated number of multiplications computed according to Sec. IV is also illustrated. The S-PIC-BDFE algorithm has a lower computational complexity compared to the GPIC-BDFE algorithm. It requires only 60.05% complex multiplications of the GPIC-BDFE algorithm. The simulation results indicate that the proposed S-PIC-BDFE algorithm is efficient for different antenna configurations.

VI. Conclusions

In this paper, a low complexity S-PIC-BDFE scheme has been proposed for the turbo detection of UD-MIMO systems. A

0018-9545 (c) 2013 IEEE. Personal use is permitted, but republication/redistribution requires IEEE permission. See http://www.ieee.org/publications_standards/publications/rights/index.html for more information.

This article has been accepted for publication in a future issue of this journal, but has not been fully edited. Content may change prior to final publication. Citation information: DOI 10.1109/TVT.2014.2298232, IEEE Transactions on Vehicular Technology

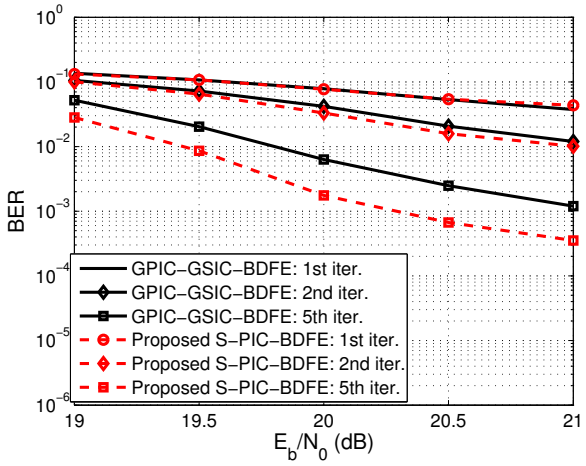

(a) BER performance

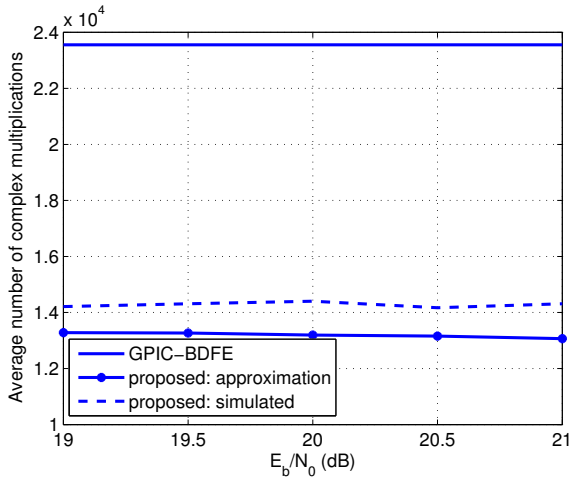

(b) Average number of complex multiplications

Fig. 7. Simulation results for a 4×2 UD-MIMO system with 16QAM modulation. Parameters are $k_l = 0.01$ and $k_u = 0.99$. The average symbol energy $E_{mean} = 1/4$ is used to estimate the upper bounds $E_m^{(u)}$. The minimum symbol energy $E_{min} = 0.2/4$ is used to estimate the lower bound $E_m^{(l)}$.

Q-ary modulated UD-MIMO system with N transmit antennas and M receive antennas was partitioned into $Q^{(N-M)}$ parallel $M \times M$ subsystems, but only a small set of the symmetric subsystems were selected to perform parallel interference cancelation and BDFE detection. In the first iteration, a new candidate set construction method was proposed by exploring the statistical properties of the received signals. For the second iteration and beyond, the candidate set was constructed by using the *a priori* information from previous iterations. Simulation results showed that the proposed S-PIC-BDFE method can achieve better BER performance than the GPIC-GSIC-BDFE method with exhaustive search, but with a lower complexity.

REFERENCES

[1] G. Karagiannis, O. Altintas, E. Ekici, G. Heijenk, B. Jarupan, K. Lin, and T. Weil, "Vehicular networking: A survey and tutorial on requirements, architectures, challenges, standards and solutions," *IEEE Communications Surveys Tutorials*, vol. 13, no. 4, pp. 584–616, fourth quarter 2011.

[2] J. L. L. Morales and S. Roy, "Spectrally efficient maximum-likelihood detection for chaotic underdetermined MIMO systems," in *IEEE Workshop on Signal Processing Systems*, Oct. 2010, pp. 186–191.

[3] Y. Oh, H. Yu, Y. Lee, and Y. Sung, "A nonlinear transceiver architecture for overloaded multiuser MIMO interference channels," *IEEE Trans. Commun.*, vol. 60, no. 4, pp. 946–951, Apr. 2012.

[4] T. Datta, N. Srinidhi, A. Chockalingam, and B. Rajan, "Random-restart reactive tabu search algorithm for detection in large-MIMO systems," *IEEE Commun. Lett.*, vol. 14, no. 12, pp. 1107–1109, Dec. 2010.

[5] N. Srinidhi, T. Datta, A. Chockalingam, and B. Rajan, "Layered Tabu search algorithm for large-MIMO detection and a lower bound on ML performance," *IEEE Trans. Commun.*, vol. 59, no. 11, pp. 2955–2963, Nov. 2011.

[6] T. Datta, N. Srinidhi, A. Chockalingam, and B. Rajan, "Low-complexity near-optimal signal detection in underdetermined large-MIMO systems," in *National Conf. Commun. (NCC) 2012*, Feb. 2012, pp. 1–5.

[7] B. M. Hochwald and S. ten Brink, "Achieving near-capacity on a multiple-antenna channel," *IEEE Trans. Commun.*, vol. 51, no. 3, pp. 389–399, Mar. 2003.

[8] L. G. Barbero and J. S. Thompson, "Extending a fixed-complexity sphere decoder to obtain likelihood information for turbo-mimo systems," *IEEE Trans.Veh. Technol.*, vol. 57, no. 5, pp. 2804–2814, Sept. 2008.

[9] K. K. Wong, A. Paulraj, and R. Murch, "Efficient high-performance decoding for overloaded MIMO antenna systems," *IEEE Trans. Wireless Commun.*, vol. 6, no. 5, pp. 1833–1843, May 2007.

[10] C. Huang, C. Wu, and T. Lee, "Geometry based efficient decoding algorithms for underdetermined MIMO systems," in *IEEE 12th International Workshop on Signal Processing Advances in Wireless Communications*, Jun. 2011, pp. 386–390.

[11] M. Damen, K. Abed-Meraim, and J. C. Belfiore, "Generalised sphere decoding for asymmetrical space-time communication architecture," *Electronics Lett.*, vol. 36, pp. 166–167, Jan. 2000.

[12] P. Dayal and M. K. Varanasi, "A fast generalized sphere decoder for optimum decoding of under-determined MIMO systems," in *41st Annu. Allerton Conf. Communication, Control, and Computing*, Oct. 2003.

[13] Z. Yang, C. Liu, and J. He, "A new approach for fast generalized sphere decoding in mimo systems," *IEEE Sig. Proc. Lett.*, vol. 12, no. 1, pp. 41–44, Jan. 2005.

[14] T. Cui and C. Tellambura, "An efficient generalized sphere decoder for rank-deficient MIMO systems," *IEEE Commun. Lett.*, vol. 9, no. 5, pp. 423–425, May. 2005.

[15] G. Romano, F. Palmieri, P. S. Rossi, and D. Mattera, "A tree-search algorithm for ml decoding in underdetermined mimo systems," in *6th Int. Symp. Wireless Commun. Syst.*, Sept. 2009, pp. 662–666.

[16] L. Wang, L. Xu, S. Chen, and L. Hanzo, "Generic iterative search-centre-shifting k-best sphere detection for rank-deficient sdm-ofdm systems," *Electronics Lett.*, vol. 44, no. 8, pp. 552–553, Apr. 2008.

[17] P. Wang and T. Le-Ngoc, "A low-complexity generalized sphere decoding approach for underdetermined mimo systems," in *IEEE Int. Conf. Commun.*, vol. 9, Jun. 2006, pp. 4266–4271.

[18] C. Qian, J. Wu, Y. R. Zheng, and Z. Wang, "Two-stage list sphere decoding for under-determined multiple-input multiple-output systems," *IEEE Trans. Wireless Commun.*, vol. 12, no. 12, pp. 6476–6487, Dec. 2013.

[19] G. J. Foschini, "Layered space-time architecture for wireless communication in a fading environment when using multiple antennas," *Bell Lab. Tech. J.*, vol. 1, pp. 41–59, 1996.

[20] D. So and Y. Lan, "Virtual receive antenna for overloaded MIMO layered space-time system," *IEEE Trans. Commun.*, vol. 60, no. 6, pp. 1610–1620, Jun. 2012.

[21] L. Bai, C. Chen, and J. Choi, "Lattice reduction aided detection for underdetermined MIMO systems: A pre-voting cancellation approach," in *2010 IEEE 71st Vehicular Technology Conference (VTC 2010-Spring)*, May. 2010, pp. 1–5.

[22] J. Wu and Y. R. Zheng, "Low complexity soft-input soft-output block decision feedback equalization," *IEEE J. Select. Areas Commun.*, vol. 26, no. 2, pp. 281–289, Feb. 2008.

[23] M. Walker, J. Tao, J. Wu, and Y. Zheng, "Low complexity turbo detection of coded under-determined MIMO systems," in *IEEE Int. Conf. Commun.*, Jun. 2011, pp. 1–5.

[24] Z. D. Luo, M. Zhao, S. Y. Liu, and Y. Liu, "Generalized parallel interference cancellation with near-optimal detection performance," *IEEE Trans. Sig. Proc.*, vol. 56, no. 1, pp. 304–312, Jan. 2008.

[25] D. Divsalar, M. K. Simon, and D. Raphaeli, "Improved parallel interference cancellation for CDMA," *IEEE Trans. Commun.*, vol. 46, no. 2, pp. 258–268, Feb. 1998.

0018-9545 (c) 2013 IEEE. Personal use is permitted, but republication/redistribution requires IEEE permission. See http://www.ieee.org/publications_standards/publications/rights/index.html for more information.

This article has been accepted for publication in a future issue of this journal, but has not been fully edited. Content may change prior to final publication. Citation information: DOI 10.1109/TVT.2014.2298232, IEEE Transactions on Vehicular Technology

[26] A. Nuttall, "Some integrals involving the Q_M function (Corresp.)," *IEEE Trans. Inf. Theory*, vol. 21, no. 1, pp. 95–96, Jan. 1975.
[27] J. H. Conway and N. J. A. Sloane, *Sphere packings, lattices and groups: Charpter 1*. New York: Springer, 1999.
[28] D. Wübben, D. Seethaler, J. Jaldén, and G. Matz, "Lattice reduction," *IEEE Sig. Proc. Magazine*, vol. 28, no. 3, pp. 70–91, May 2011.

Chen Qian received his B.S. degree in Electronic Engineering from Tsinghua University, Beijing, China in July 2010. In September 2010, he has been a Ph. D. candidates at the Department of Electronic Engineering of Tsinghua University. His research interests include large-scale MIMO, detection algorithm of MIMO systems, channel coding and modulation.

Jingxian Wu (S'02-M'06) received the B.S. (EE) degree from the Beijing University of Aeronautics and Astronautics, Beijing, China, in 1998, the M.S. (EE) degree from Tsinghua University, Beijing, China, in 2001, and the Ph.D. (EE) degree from the University of Missouri at Columbia, MO, USA, in 2005. He is currently an Assistant Professor with the Department of Electrical Engineering, University of Arkansas, Fayetteville. His research interests mainly focus on wireless communications and wireless networks, including ultra-low power communications, energy efficient communications, high mobility communications, and cross-layer optimization, etc. He is an Associate Editor of the IEEE TRANSACTIONS ON WIRELESS COMMUNICATIONS, an Associate Editor of the IEEE ACCESS, and served as an Associate Editor of the IEEE TRANSACTIONS ON VEHICULAR TECHNOLOGY from 2007 to 2011. He served as a co-chair for the 2012 Wireless Communication Symposium of the IEEE International Conference on Communication, and a co-chair for the 2009 Wireless Communication Symposium of the IEEE Global Telecommunications Conference. Since 2006, he has served as a Technical Program Committee Member for a number of international conferences, including the IEEE Global Telecommunications Conference, the IEEE Wireless Communications and Networking Conference, the IEEE Vehicular Technology Conference, and the IEEE International Conference on Communications.

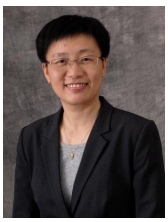

Yahong Rosa Zheng (SM'07) received the B.S. degree from the University of Electronic Science and Technology of China, Chengdu, China, in 1987, and the M.S. degree from Tsinghua University, Beijing, China, in 1989, both in electrical engineering. She received the Ph.D. degree from the Department of Systems and Computer Engineering, Carleton University, Ottawa, Canada, in 2002. She was an NSERC Postdoctoral Fellow from Jan. 2003 to April, 2005 at University of Missouri-Columbia. In fall 2005, she joined the Department of Electrical and Computer Engineering at the Missouri University of Science and Technology where, currently, she is an Associate Professor. Her research interests include array signal processing, wireless communications, and wireless sensor networks. She has served as a Technical Program Committee (TPC) member for many IEEE international conference, including IEEE Vehicular Technology Conference, IEEE GlobeCom, and IEEE ICC, and IEEE Wireless Communications and Networking Conference, etc. She served as Wireless Communications Symposium co-chair for ICC 2014 and Globecom 2013. She also served as an Associate Editor for IEEE TRANSACTIONS ON WIRELESS COMMUNICATIONS for 2006-2008. She is currently Associate Editor for IEEE TRANSACTIONS ON VEHICULAR TECHNOLOGY. She has been a Senior Member of the IEEE since 2007. She is the recipient of an NSF CAREER award in 2009.

Zhaocheng Wang (SM'10) received his B.S., M.S. and Ph.D. degrees from Tsinghua University in 1991, 1993 and 1996, respectively. From 1996 to 1997, he was with Nanyang Technological University (NTU) in Singapore as a Post Doctoral Fellow. From 1997 to 1999, he was with OKI Techno Centre (Singapore) Pte. Ltd., firstly as a research engineer and then as a senior engineer. From 1999 to 2009, he worked at SONY Deutschland GmbH, firstly as a senior engineer and then as a principal engineer. He is currently a Professor at the Department of Electronic Engineering, Tsinghua University. His research areas include wireless communications, digital broadcasting and millimeter wave communications. He holds 33 granted US/EU patents and has published over 100 technical papers. He has served as technical program committee co-chair/member of many international conferences. He is a Fellow of the Institution of Engineering and Technology.

0018-9545 (c) 2013 IEEE. Personal use is permitted, but republication/redistribution requires IEEE permission. See http://www.ieee.org/publications_standards/publications/rights/index.html for more information.